Extrapolation of Radio Sources to 31 GHz with the S^3-SEX

T.Chantavat

ThEP's CRL, NEP, The Institute for Fundamental Study, Naresuan University, Phitsanulok 65000, Thailand
Thailand Center of Excellence in Physics, Ministry of Education, Bangkok 10400, Thailand
Corresponding author. E-mail: teeraparbc@nu.ac.th

Abstract

Point sources have long been known as major contaminants of Cosmic Microwave Background (CMB) experiments especially on small angular scales. In order to understand the anisotropies in the CMB on small scales, it is necessary to understand point sources contained in the field of observations. Bright sources, which can be detected with high significance in CMB maps are typically accounted for by masking a small area around the source position during the estimation of the CMB angular power spectra, C_ℓ. On the other hand, undetected point sources and hence unsubtracted will provide a contribution to the map and so to C_ℓ. We shall use the S^3-SEX simulation to study sub-populations of radio sources that are most likely to have an inverted spectrum, and hence contribute to the source counts at high frequencies.

Keywords**:** Galaxies: Starburst – Galaxies: Luminosity Function – Galaxies: Radio Continuum – Cosmology: Large-scale Structure

1. Introduction

Point sources have long been known as major contaminants of Cosmic Microwave Background (CMB) experiments especially on small angular scales (See e.g. BOOMERanG [1], MAXIMA [2], ACBAR [3], CBI [4]). In order to understand the anisotropies in the CMB on small scales, it is necessary to understand point sources contained in the field of observations. Bright sources, which can be detected with high significance in CMB maps, are typically accounted for by masking a small area around the source position during the estimation of the CMB angular power spectra, C_ℓ. On the other hand, undetected point sources and hence unsubtracted will provide a contribution to the map and so to C_ℓ. Various experiments, especially at frequencies around 30 GHz, such as CBI [5], SZA [6], and VSA [7], have observed both the CMB angular power spectrum on small scales and made independent estimations of the point source contamination in their fields.

To study radio point sources, blind radio observations at different frequencies are required. There is a wealth of information on radio surveys in the frequencies around ~ 1 GHz. Within this range, the largest mJy survey is the NRAO-VLA Sky Survey (NVSS) [8] which covers about 80% of the sky. Table 1 shows radio continuum surveys with sky coverage larger than 25% from 74 MHz to 94 GHz from the VLA Low-Frequency Sky Survey (VLSS) [9], Westerbork Northen Sky Survey (WENSS) [10], Sydney University Molongo Sky Survey (SUMSS) [11], NRAO VLA Sky Survey (NVSS) [8], single-dish PMN and GB6 surveys [12 - 13], AT20G [14] and WMAP extragalactic source catalogue [15].

Table 1: The radio continuum survey with the sky coverage larger than 25% from 74 MHz to 94 GHz

Survey	Effective Frequency (GHz)	Sensitivity Limit (mJy)
VLSS	0.074	500
WENSS	0.325	18
SUMSS	0.843	5
NVSS	1.4	2.5
PMN/GB6	4.85	35
AT20G	20	60
WMAP	23, 33, 40, 60, 94	1,000

Some other deep mJy surveys, but having smaller area coverage, are at 4.86 GHz [16], 8.5 GHz [17] and 15.2 GHz [18] but there is currently no such deep, wide-area blind survey above 15.2 GHz. The main reason is that wide-area observations at higher radio frequencies are impractical due to the small beam size of present telescopes. In the absence of high frequency source catalogues, removal of point sources from the CMB has to rely upon the extrapolation and interpretation of sources at much lower frequencies. The CMB observed frequencies are in the range 25 - 100 GHz therefore extrapolations of the point source power spectrum from low frequencies (1.4 - 15.2 GHz) to higher frequencies can become uncertain and inaccurate as the properties of

point sources are not well understood or certain types of radio population become dominant. The sources that have rising flux densities at higher frequencies are collectively known as *inverted-spectrum sources*. Study of inverted-spectrum sources is important to fully understand the effect of extragalactic radio contamination. These sources may go undetected in low frequency surveys but be bright enough at higher frequencies to be of concern. Attempts to study the inverted-spectrum populations have been done by following-up surveys of selected inverted-spectrum sources at low frequencies (See for example [19]).

The Cosmic Background Imager (CBI), one of the CMB experiments on small scales, observed a ~ 3 - σ excess in the angular power spectrum at multipole moment, ℓ ~ 2500 [4]. The excess can be explained by the Sunyaev-Zel'dovich Effect (SZE) [20]; however, σ_8 required to give the amount of the SZE excess is marginally higher than σ_8 derived from the CMB. Recently, the Sunyaev-Zel'dovich Array (SZA) has published radio source counts at 31 GHz which show a higher number of sub-mJy sources than those derived by CBI [5], but are in good agreement with the higher 10 - 20 mJy counts determined by the VSA at 33 GHz. Having a higher radio source power spectrum in the excess would alleviate the tension in the values of σ_8. However, one must be careful when interpreting these results. The CBI independently observed all sources in the NVSS catalogues at 31 GHz using the GBT [5] and used the resulting spectral index distribution to statistically determine the sub-mJy counts at 31 GHz. They therefore had essentially a large 'survey area' but determined by the much lower 1.4 GHz NVSS survey. SZA conducted a blind 31 GHz survey but over a much smaller area reaching flux limit of ~ 1 mJy. The VSA undertook a blind survey at 15 GHz down to ~ 10 mJy which was then followed up by observations at 33 GHz. Hence all three surveys have potential problems whether due to a small statistical sample or extrapolations over large frequency ranges. The possible discrepancy between them at low flux levels and the dependence on selection effects is the subject of this chapter.

In this paper, we use the Square Kilometre Array Design Studies (SKADS) Simulated Skies Simulation of EXtragalactic radio continuum, S^3-SEX[1] [21], to study the CBI radio source subtraction process. The S^3-SEX is a computer simulation of a 20 × 20 deg^2 patch of a sky out to $z = 20$, and down to a flux density of 10 nJy[2] at 151, 610 MHz, 1.4, 4.86 and 18 GHz frequency channels. The results of the SKADS simulation match various observations up to 18 GHz. However, there is no deep survey beyond 18 GHz and hence there is still a freedom of modifying the S^3-SEX at frequencies beyond 18 GHz. The advantage of the SKADS catalogue is that the radio sources are characterised into different populations (normal galaxies, star-burst galaxies, radio-quiet AGNs, FRI's, FRII's and GPS's). Some of the sources are well-studied and have a specific spectral index whereas the others are less known and have less defined spectral index distributions. By studying how the spectral index distribution of each of the populations can be varied to match e.g. the SZA observations, we can narrow down the potential populations which have inverted spectral index and give rise to the CMB power spectrum seen by CBI, SZA and VSA.

We begin in Section 2 with models of radio source extrapolation. In Section 3, we describe the SKADS characterisation of the major radio source populations. Based on the model done by the SKADS team, we look at how the model matches the recent deep survey source counts at high frequency and also the extrapolation to the CBI operating frequency at 31 GHz in Section 4. Conclusions are given in Section 5.

2. Power Spectrum of Extragalactic Radio Source

Point Sources are the largest astrophysical foreground in the CMB data along with Sunyaev-Zel'dovich effect on small scales. Their angular power spectrum, when assuming a Poissonian distribution, increases as ℓ^2 whereas the CMB power spectrum decreases with ℓ due to Silk damping effect. Hence, the point source contamination is critical at high ℓ. The point source power spectrum can be estimated if the flux distribution of the sources is known at that frequency.

In this section, the standard theoretical formalism of radio source populations is over-viewed. The concepts of frequency spectral index, differential source count and normalised differential source count are introduced which are commonly used in contemporary literature.

2.1 Flux Density Spectrum

The standard method used to extrapolate flux densities at one frequency to other frequencies can be achieved by assuming that the variation of the flux density across the frequency domain is a power-law. The spectral index[3] α is defined as

$$S(\nu;\alpha) = S_0 \times \left(\frac{\nu}{\nu_0}\right)^{\alpha}, \qquad (1)$$

where S_0 is the flux density at the reference frequency ν_0. This method assumes that the spectral index and the distribution of the spectral index characterize all the point source populations present. However, this simple power law extrapolation will fail if there are some classes of population whose flux density suddenly become important at the extrapolated frequency.

[1] Available online at http://s-cubed.physics.ox.ac.uk

[2] 1 Jy (Jansky) = 10^{-26} W Hz^{-1} m^{-2} or 10^{-23} erg cm^{-2} s^{-1} Hz^{-1}.

[3] Some literature define the spectral index, α, as $S \equiv S_0(\nu/\nu_0)^{-\alpha}$.

2.2 Source Count

We define the differential number count at a certain frequency ν, $n_\nu(S)$, as the number of sources per unit flux density per steradian[4], $n_\nu(S) \equiv \mathrm{d}N/\mathrm{d}S$ at frequency ν. The differential source count per unit area as a function of flux, $\mathrm{d}N/\mathrm{d}S$, is typically described by a power law, i.e.,

$$n_\nu(S) \equiv \left(\frac{dN}{dS}\right)\Big|_\nu = N_0 \left(\frac{S}{S_0}\right)^\gamma, \qquad (2)$$

where N_0 is a normalisation parameter per unit area, S is the source flux, and γ is the power law index. From (1), the predicted differential source count at frequency ν is

$$n_\nu(S) = \int_{-\infty}^{\infty} n\left[\left(\frac{\nu}{\nu_0}\right)^\alpha S, \nu_0\right] P(\alpha)\mathrm{d}\alpha, \qquad (3)$$

where $P(\alpha)$ is the observed spectral index distribution which is assumed independent of flux density. The normalised differential source count is the normal differential source count divided by $S^{-2.5}$. The factor is derived from the fact that if the Universe is static and the radio sources are distributed equally, the differential source count will scale as $S^{-2.5}$.

2.3 Angular Power Spectrum

The angular power spectrum of point sources, if we assume a Poisson distribution, is independent of ℓ and is given by

$$C_l^{\mathrm{src}} = X_{\mathrm{src}} \times \left[\frac{2k_\mathrm{B}}{c^2}\left(\frac{k_\mathrm{B}T_\mathrm{CMB}}{h}\right)^2 \frac{x^4}{(e^x-1)^2}\right]^{-2}, \qquad (4)$$

where C_ℓ is the power spectrum of the residual sources below $S_{\max}$ and $x \equiv h\nu/k_\mathrm{B}T_\mathrm{CMB}$ is the frequency dependent term. X_{src} is given by

$$X_{\mathrm{src}} = \int_0^{S_{\max}} \mathrm{d}S S^2 \frac{\mathrm{d}N}{\mathrm{d}S}, \qquad (5)$$

whrere $\mathrm{d}N\backslash\mathrm{d}S$ is the differential source count defined in (2). X_{src} is known as the *residual power spectrum*. The CMB band power is normally express in terms of $\ell(\ell+1)C_\ell / 2\pi$. Hence, the point source contribution to the CMB has an ℓ^2 dependent and is why point sources become important on small scales.

3. The SKADS Simulated Skies (S^3) Radio Source Populations

The S^3-SEX is the first attempt to create a semi-emperically generated radio-continuum 20 × 20 deg^2 patch of a sky by incorporating all known radio source observations at GHz frequency ranges, down to a faint flux level of ~ 10 nJy. In order to extrapolate the radio sources to such low flux densities accurately, a complete understanding of different radio source populations is needed. In addition to extrapolating to lower flux densities, the simulation allows one to extrapolate the individual population to a different frequency by providing five different frequency channels. It is therefore an ideal catalogue for us to use to test our hypotheses of source variations at high frequencies. In this chapter, we follow a classification of radio sources based on the SKADS simulation [21].

Star-Forming Galaxies

The main mechanism for radio emission in galaxies not dominated by Active Galactic Nuclei (AGN) is mainly *synchrotron radiation*, which is caused by accelerated charged particles moving through magnetic fields in star-forming regions, at low frequencies and *free-free radiation*, which is caused by decelerated charged particles, at higher frequencies. They can be sub-divided into two classes.

- **Normal Star-Forming Galaxies**
  Normal star-forming galaxies emit strong radio continuum emission, either free-free radiation (Bremsstrahlung) or synchrotron radiation in region of strong electromagnetic field.
- **Star-Burst Galaxies**
  Star-burst galaxies have an exceptionally high rate of star formation in comparison to usual star-forming galaxies. They exhibit strong radio emission from star-forming regions which are expected as supernova remnants. Star-burst galaxies can be disk galaxies or irregular galaxies.

Radio-Quiet Quasar

Quasi-stellar objects (quasars) are a type of AGN which have a compact region at the centre of a massive galaxy. Quasars are powered by an accretion disc around the black hole. They always show strong optical emission with both narrow and broad lines and usually are more luminous than normal radio galaxies. The distinction is usually expressed in terms of a limiting optical magnitude. Radio Quiet Quasars (RQQ's) have strongly accreting disks yet lack the extensive 100 kpc scale jets that steadily transport away energy and angular momentum from the nuclei of radio-loud quasars and radio galaxies. However, the luminosity of the core of RQQ's can be as high as that of the core of radio-loud quasars.

Radio-loud AGN

Radio-loud AGNs are sub-divided into two classes based on the classification by B. L. Fanaroff and J. M. Riley [22]. They found that the relative positions of the regions of high and low surface brightness in the lobes of extragalactic radio sources are correlated with their radio luminosity. The

[4] sometimes as per deg^2.

conclusion was based on 57 radio galaxies and quasars in the 3CR catalogue at 178 MHz which were resolved at 1.4 GHz and 5.0 GHz. The sources were classified using the ratio of the distance between two opposite highest surface brightness spots and the distance up to the total extent of the sources at their lowest surface brightness, R_{FR}. The radio sources which have $R_{\mathrm{FR}} < 0.5$ were placed in Class I while the sources which have $R_{\mathrm{FR}} > 0.5$ were placed in Class II. Various properties of the two classes are different which indicates the link between the luminosity and the way in which energy is transported from the core to the outer parts.

- **FRI**
  AGNs of this class have their lowest surface brightness regions further from the central core. The extended lobes fade without clear end. FRI sources are associated with bright, large galaxies that have a flatter light distribution than an average elliptical galaxy. They are often located in rich clusters with extreme X-ray emitting gas. FRI sources are associated with BL Lac objects, characterised by optically-featureless continua.
- **FRII**
  The radio sources of this class have more defined boundaries of their extended lobes, but are expected to decrease in surface brightness as they age and grow in size. They can be easily undetected at high redshift due to the very low level of central AGN-like activity. They can be seen as flat-spectrum.

GHz-Peaked Spectrum - GPS

GHz-Peaked Spectrum (GPS) sources are extra-galactic radio sources which have their radio spectrum peaking around 0.5 - 10.0 GHz. The physical mechanism of GPS sources is still unclear. However, there are two possible scenarios that have been proposed: (i) the synchrotron self-absorption caused by dense plasma within the source; (ii) the free-free absorption caused by an external source. GPS sources are often associated with either quasars or galaxies. They are characterised by having a positive spectral index at low frequencies and a negative spectral index at high frequencies. GPS sources are associated with either quasars or galaxies, however galaxies are a more common host of GPS sources than quasars. Similar to many other extra-galactic radio sources, GPS sources are subjected to time variability.

At flux densities $S \geq 1$ mJy, the radio source population is dominated by radio-loud AGNs (FRI, FRII and GPS sources). However, at flux densities $S \leq 1$ mJy, the radio number counts significantly flatten [23 - 24]. This indicates either a sudden change in evolution properties at low flux densities, or more likely, an emergence of a new sub-population dominated at low flux densities such as normal, star-burst galaxies and RQQ's.

4. SKADS Sources Extrapolation to 31 GHz

We utilised the SKADS simulation of radio sources to understand the implications of the CBI source selection effects and to understand how a change in the spectral property of one of the radio populations listed in Section 3 may result in an excess of point sources over that currently predicted.

4.1 CBI Selection Effect

Our aim is to utilise the SKADS catalogue with some extrapolation methods to explain the discrepancies between the CBI and SZA result at low flux. First, we replicate the CBI source selection by selecting all the radio sources which have flux densities $S < 3.4$ mJy at 1.4 GHz (complete flux limit for the NVSS survey). The spectral index probability distribution function derived from the SKA simulation is shown in Figure 1. Normal galaxies and star-burst galaxies have $\alpha_{4.86}^{18.0}$ peaking around -0.5 with a tail of distribution towards inverted spectra sources. They both have effectively the same distribution. However, normal galaxies are more populous than star-burst galaxies. All the other populations except for normal galaxies and star-burst galaxies have a well-defined spectral index. RQQs have a spectral index of -0.7. FRI and GPS sources have spectral index of -0.75. The GPS sources spectral index has already declined between 4.86 - 18.00 GHz. There are no FRII sources because they are extremely rare, luminous and are ruled out by the CBI selection criterion. In order to estimate the number of sources at 31 GHz, we then need to extrapolate the source count from one of the SKADS frequencies. We define three extrapolation scenarios as follows:

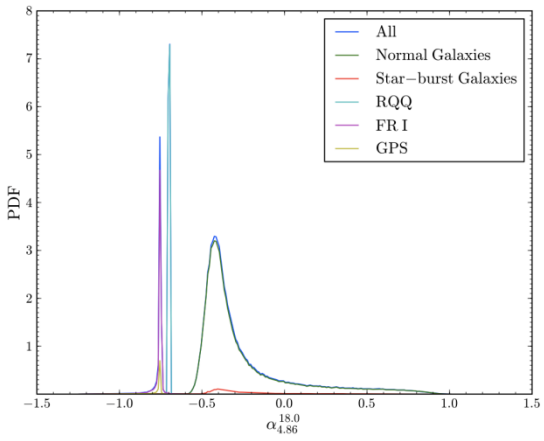

Figure 1. The spectral index probability distribution from SKADS simulation with CBI selection criterion

- **Linear Extrapolation (LE):**
  In this scenario, we linearly extrapolate the source count at 4.86 GHz to 31 GHz using the spectral index between 4.86 - 18.0 GHz from the SKADS catalogue. It is arguable whether 1.4 GHz is a preferable choice of base frequency in order to replicate the CBI method. However, there are some drawbacks in this choice of frequency. Firstly, there are some radio sources, mainly GPS sources, which have a rising spectral index at low frequencies but a declining spectral index at high frequencies. Linearly extrapolating these peaked spectrum sources at low frequency may over-predict the source count at 31 GHz. Therefore it is preferable to use the two highest frequency channels in the catalogue which are 4.86 and 18.0 GHz respectively. Secondly, there are many deep observations at 4.86 GHz [16, 25 - 26] down to a few 10 μJy. Having the base frequency at 4.86 GHz gives us better constraints on low flux populations. We note that the 1.4 and 4.86 GHz SKADS source counts both accurately match the observed point source populations down to sub-mJy levels.
- **Global Extrapolation (GE):**
  From the SKADS catalogue, we derive a spectral index distribution from 4.86 to 18.0 GHz, $P(\alpha_{4.86}^{18.0})$. From $P(\alpha_{4.86}^{18.0})$, we use (1) to estimate the source contribution at 31 GHz. This method assures a common spectral index distribution for all source populations.
- **Individual extrapolation (IE):**
  The last scenario is the case where the sources are extrapolated to 31 GHz according to their own population spectral index distribution. This method is similar to GE except that we derive the distribution for each population type separately (See Figure 1.).

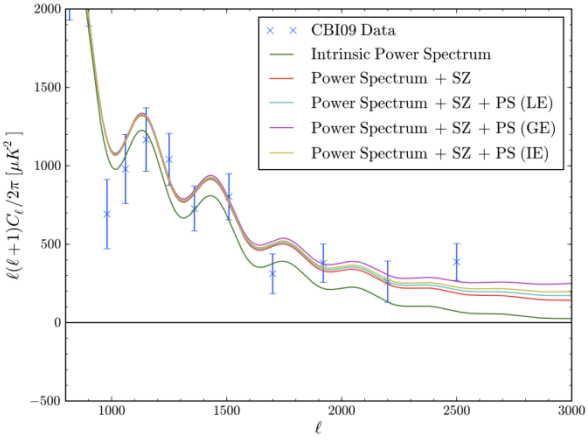

Figure 2. CMB bandpower with CBI data

Figure 2 shows the WMAP5 angular power spectrum, the power spectrum including SZ contribution as determined from [27] and the power spectrum with point sources contribution from all the three scenarios. The intrinsic power spectrum was calculated using WMAP5 maximum likelihood parameters [28] using a publicly available CAMB code [29]. We estimate the point source angular power spectrum using Figure 3 by assuming the CBI flux limit of 1 mJy.

From Figure 2, all the extrapolation methods lie below the observed band power at ℓ = 2,500 within 2 - σ level. The value of $C_\ell^{\rm src}$ for LE, GE and IE are 21.1, 75.5 and 38.6 nK^2 respectively while Mason *et al.* 2009 [5] has an estimated $C_\ell^{\rm src} = 44 \pm 14$ nK^2 for CBI. The IE and LE methods yield similar results demonstrating that the shape of the spectral index distribution does not vary significantly in the two extrapolation methods. The GE case, which is surely an incorrect extrapolation method, yields the highest point source power spectrum due to the fact that FRI and RQQ sources, which intrinsically have a declining spectral index, can be confused with normal galaxies and extrapolated to 31 GHz with higher or flat spectral index. A good agreement of our estimated $C_\ell^{\rm src}$ from the IE method and the CBI result reflects a good careful statistical treatment of point sources from the CBI team given all information that we currently know from low frequency surveys. However, comparing the radio source estimation from extrapolation of low frequencies with blind surveys at 31 GHz e.g. by SZA, there is still clearly a discrepancy on mJy populations (See Figure 4 in [6]).

4.2 Shiftling of Inidividual Spectral Index Distribution

Next, we took an alternative approach to see how different sources could potentially contribute to the excess based on an assumption that the spectral index property of the populations is allowed to alter at high frequencies where there is no deep survey data to constrain this. Some of the sources are well-known and have a well-defined physical mechanism that drives their radiation, while the others are less known and still under debate. We selected all the sources above $S > 1$ μJy at 1.4 GHz from SKADS simulation without any high flux cut-off. The spectral index distribution of $\alpha_{4.86}^{18.0}$ is derived from the catalogue. Similar to the IE extrapolation method in Section 4.1, we extrapolate each source to the CBI operating frequency of 31.0 GHz from their individual spectral index distribution. We compare our result with observational data constraint from CBI [30] at 31 GHz, SZA [6] at 31 GHz, VSA [7] at 33 GHz and CBI/GBT [5] 31 GHz as shown in Figure 3. As described before in Section 1, the VSA and CBI/GBT results are from 31 GHz observation of lower frequency selected source. The SZA and CBI results are from blind surveys at flux limit of ~ 1 mJy and ~ 10 mJy respectively. The errors shown in the figure

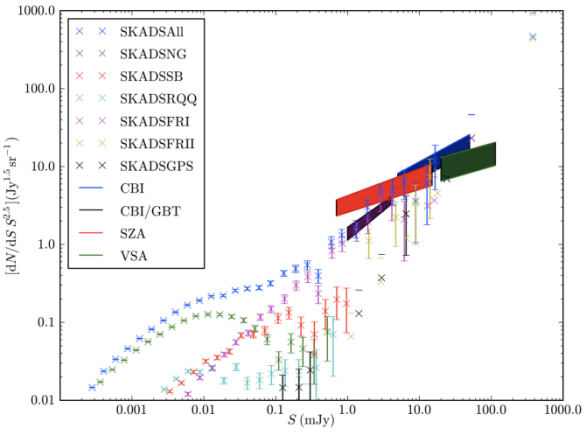

Figure 3. SKADS sources extrapolation to 31 GHz in comparison with observational constraints

are Poisson errors.

Our extrapolated number counts match the result from CBI/GBT while SZA observes higher number of radio sources between 1 - 10 mJy. In Section 4.1, we have shown that all the extrapolation methods given the information of constraints we know from deep low frequency surveys cannot give an excess in number count as shown by SZA [6]. To reconcile the discrepancy without introducing a new type of population, the spectral property of the sources at high frequency end has to be adjusted to match the observations. To address our question of possible deviation of spectral index distribution at high frequency, we shifted the individual spectral index distribution by an extreme value of $\Delta\alpha_{4.86}^{18.0} = 0.9$ and extrapolate to 31.0 GHz in order to see how much of an effect each type of population could potentially be in the flux range of 1 - 10 mJy. Figure 4 shows the deviation in number count in comparison to the standard extrapolation method for each population.

- **Normal galaxies**
  Normal galaxies dominate the low-flux population whose number density peaks at ≈ 0.1 μJy at 4.86 GHz. The required spectral index for this population to have an impact at flux density ~ 1 mJy at 31 GHz would be ≈ 0.75. The radiation from normal galaxies derive from synchrotron radiation and free-free radiation which has intrinsically declining spectral index. Such a high rising spectral index is improbable for normal galaxies.
- **Star-burst galaxies**
  Star-burst galaxies have a similar mechanism to normal galaxies with an exception of higher rate of star formation. As a result, they produce higher flux densities than normal galaxies but are less populous. Having an intrinsically declining spectral index, it is not possible for star-burst galaxies to account for an excess at 1 mJy at 31 GHz.
- **RQQ's**
  Similar to normal galaxies and star-burst galaxies, radio-quiet quasars produce low flux densities and have a spectral index $\alpha_{4.86}^{18.0} \approx$ -0.7 which make them an unlikely choice to have any impact around ~ 1 mJy at 31 GHz.
- **FRI AGN's**
  Shifting the spectral index of FRI population with $\Delta\alpha_{4.86}^{18.0} = 0.9$ fits the SZA result but it breaks the high-flux constraint. The required $\Delta\alpha_{4.86}^{18.0}$ to actually sufficently boosts the source count at 1 mJy is around 0.6 which corresponds to a flat spectrum FRI source. A refined model of FRI that equivalently produces a high flux cut-off could be made to fit the data without breaking the high-flux constraint. An example model could be an enhancement of high redshift FRI sources.
- **FRII AGN's**
  FRII active galactic nuclei galaxies already produce a high flux density with a declining spectral index. Fine-tuning the value of $\Delta\alpha_{4.86}^{18.0}$ can bring the population to peak around 1 mJy at 31 GHz. However, they are rare and such luminous sources can easily be detected at low frequencies. In addition, CBI observed all the radio sources from NVSS survey in the field of observation from their follow-up survey [5], making FRII an unlikely choice of population.
- **GPS**
  The result shows that GPS sources have little effect due to their scarceness even though their physical mechanism is still under debate.

5. Conclusions

The S^3-SEX is a 20 × 20 deg^2 simulated patch of a sky based on all the available data and models to-date which matches remarkably well against observations in many different frequencies from 151 MHz to 15.2 GHz. However, beyond 15.2 GHz the radio sources are hardly and sparsely constrained. The main target for the next generation radio surveys will be to attempt to constrain lower flux limits at both low frequencies and high frequencies as well as filling in gaps in radio frequencies beyond 20 GHz. Pushing the flux limit down at low frequencies will beneficially aid us in understanding the low-flux population and modelling of spectral properties of radio sources. The inconsistency in radio number counts between the CBI and SZA is an alarming sign of a need to redefine our model of radio sources and as a prerequisite step for upcoming CMB temperature and polarisation surveys such as the ESA PLANCK mission. We utilized the SKADS sky simulation to

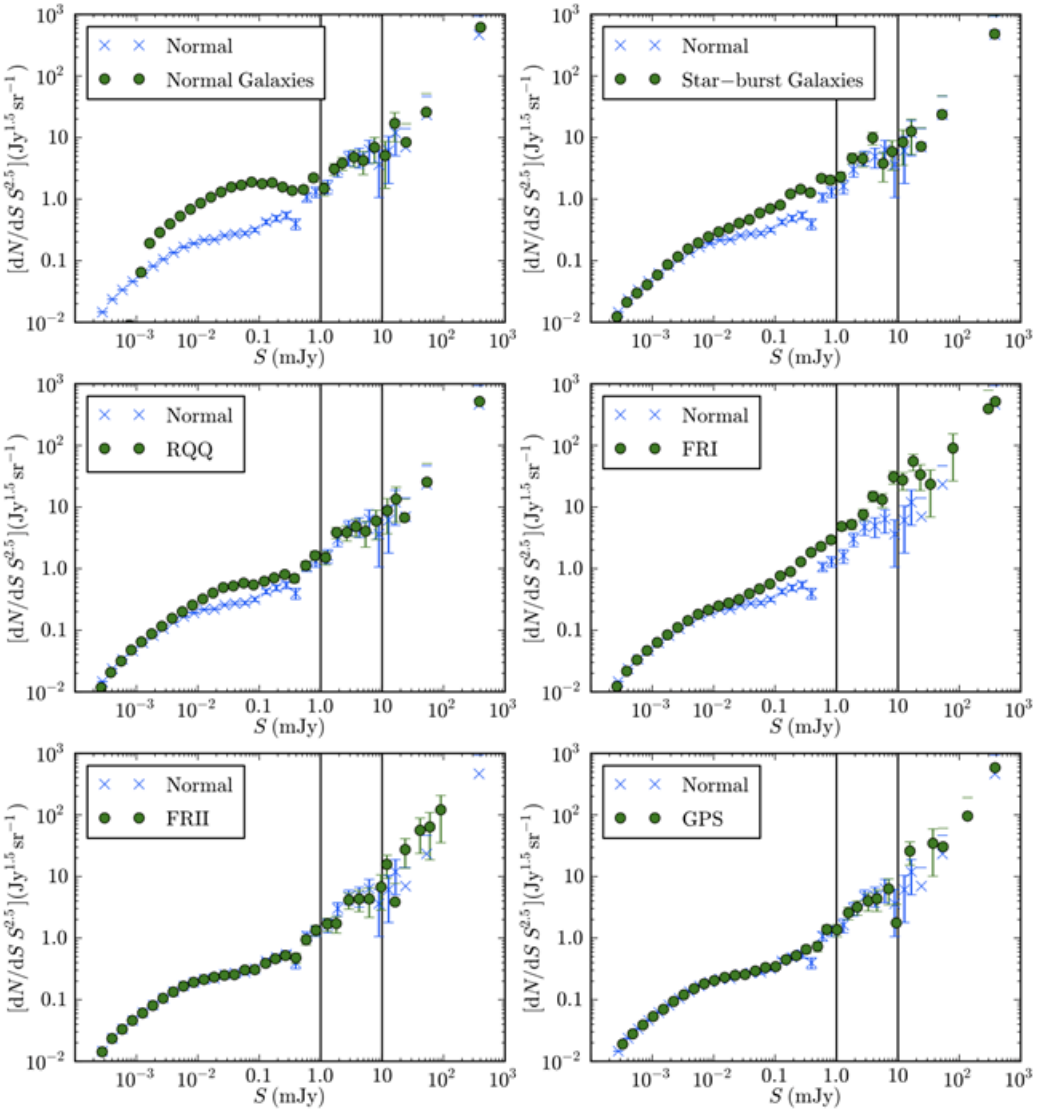

Figure 4. Comparison of radio source number counts at 31 GHz between extrapolation from standard and shifted spectral index distribution for each of the SKADS radio sources. The vertical bands show the mismatched flux density range between the SZA and CBI observation.

address this problem. There had been speculation that the CBI selection effect which leads to the discrepancy in the CMB power spectrum at high ℓ. However, our result is in good agreement with that of CBI and, hence, selection effects may not be an entire source of the mismatch. A simple first order perturbation of spectral index distribution of different radio populations simply could not account for the discrepancy. A possible solution is an amendment to the sources's space density model. FRI source models could potentially be adjusted to match the SZA data due to their high space density and relevant flux density range. Further investigation of redshift effects and of space density i.e. the luminosity function, is needed to accurately model point sources at high redshifts.

Acknowledgments

T. Chantavat would like to thank to A. C. Taylor and M. E. Jones for some fruitful discussion to the project.

References

1. B. P. Crill *et al.*, "A Balloon-born Millimeter-Wave Telescope and Total Power Receiver for Mapping Anisotropy in the Cosmic Microwave Background", ApJS **148** (2003), 527.
2. M. E. Abroe *et al.*, "Correlations between the Wilkinson Microwave Anisotropy Probe and MAXIMA Cosmic Microwave Background Anisotropy Maps", ApJ **605** (2004) 607.

3. C. L. Kuo *et al.*, "Improved Measurements of the CMB Power Spectrum with ACBAR", ApJ **664** (2007) 687.
4. J. L. Sievers *et al.*, "Cosmological Results from Five Years of 30 GHz CMB Intensity Measurements with the Cosmic Background Imager", ArXiv e-prints, arXiv:**0901**.454
5. B. S. Mason *et al.*, "A 31 GHz Survey of Low-Frequency Selected Radio Sources", ApJ **704** (2009), 1433.
6. S. Muchovej et al.., "Radio Sources from a 31 GHz Sky Survey with the Sunyaev- Zel'dovich Array", ApJ **716** (2010), 521.
7. K. A. Cleary *et al.*, "Source Subtraction for the Extended Very Small Array and 33-GHz Source Count Estimates", MNRAS **360** (2005), 340.
8. J. J. Condon *et al.*, "The NRAO VLA Sky Survey", AJ **115** (1998), 1693.
9. A. S. Cohen *et al.*, "The VLA Low-Frequency Sky Survey", AJ **134** (2007), 1245.
10. R. B. Rengelink *et al.*, "The Westerbork Northern Sky Survey (WENSS), I", A&AS **124** (1997), 259.
11. D. C.-J. Bock, M. I. Large, and E. M. Sadler., "SUMSS: AWide-Field Radio Imaging Survey of the Southern Sky. I. Science Goals, Survey Design, and Instrumentation", AJ **117** (1999), 1578.
12. M. R. Griffith and A. E. Wright, "The Parkes-MIT-NRAO (PMN) Surveys. I – The 4850 MHz Surveys and Data Reduction", AJ **105** (1993), 1666.
13. P. C. Gregory, W. K. Scott, K. Douglas, and J. J. Condon, "The GB6 Catalog of Radio Sources", ApJS **103** (1996), 427.
14. R. Ricci *et al.*, "First Results from the Australia Telescope Compact Array 18-GHz Pilot Survey", MNRAS **354** (2004), 305.
15. B. Gold *et al.*, "Seven-Year Wilkinson Microwave Anisotropy Probe (WMAP) Observations: Galactic Foreground Emission", ApJS **192** (2011), 15.
16. E. B. Fomalont *et al.*, "The Micro-Jansky Radio Source Population at 5 GHz", AJ **102** (1991), 1258.
17. E. B. Fomalont *et al.*, "The Microjansky Sky at 8.4 GHz", AJ **123** (2002), 2402.
18. E. M. Waldram *et al.*, ". 9C Continued: a Radio-source Survey at 15 GHz", ArXiv e-prints, arXiv:0908.0066
19. E.M. Sadler *et al.*, "The Extragalactic Radio-Source Population at 95GHz", MNRAS **358** (2008), 1656.
20. M. Birkinshaw., "The Sunyaev-Zel'dovich Effect", Phys. Rep. **310** (1999), 97.
21. R. J. Wilman *et al.*, "A Semi-Empirical Simulation of the Extragalactic Radio Continuum Sky for next Generation Radio Telescopes", MNRAS **388** (2008), 1335.
22. B. L. Fanaroff and J. M. Riley, "The Morphology of Extragalactic Radio Sources of High and Low Luminosity", MNRAS **167** (1974), 31P.
23. J. J. Condon, "The 1.4 Gigahertz Luminosity Function and its Evolution", ApJ **338** (1989), 13.
24. E. A. Richards, "The Nature of Radio Emission from Distant Galaxies: The 1.4 GHz Observations", ApJ **533** (2000), 611.
25. P. Ciliegi *et al.*, "A Deep VLA Survey at 6 cm in the Lockman Hole", A&A **398** (2003), 901.
26. I. Prandoni *et al.*, "The ATESP 5 GHz Radio Survey. I. Source Counts and Spectral Index Properties of the Faint Radio Population", A&A **457** (2006), 517.
27. E. Komatsu and U. Seljak, "The Sunyaev-Zel'dovich Angular Power Spectrum as a Probe of Cosmological Parameters", MNRAS **336** (2002), 1256.
28. J. Dunkley *et al.*, "Five-Year Wilkinson Microwave Anisotropy Probe Observations: Likelihoods and Parameters from the WMAP Data.", ApJS **180** (2009), 306.
29. A. Lewis, A. Challinor, and A. Lasenby, "Efficient Computation of Cosmic Microwave Background Anisotropies in Closed Friedmann-Robertson-Walker Models", ApJ **538** (2000), 473.
30. B. S. Mason *et al.*, "The Anisotropy of the Microwave Background to ℓ = 3500: Deep Field Observations with the Cosmic Background Imager", ApJ **591** (2003), 540.